

# Bacterial adhesion to glass and metal-oxide surfaces

Baikun Li<sup>a,\*</sup>, Bruce E. Logan<sup>b</sup>

<sup>a</sup> Environmental Engineering Program, The Pennsylvania State University at Harrisburg, Middletown, PA 17057, USA

<sup>b</sup> Department of Civil and Environmental Engineering, The Pennsylvania State University, University Park, PA 16802, USA

Accepted 4 May 2004

## Abstract

Metal oxides can increase the adhesion of negatively-charged bacteria to surfaces primarily due to their positive charge. However, the hydrophobicity of a metal-oxide surface can also increase adhesion of bacteria. In order to understand the relative contribution of charge and hydrophobicity to bacterial adhesion, we measured the adhesion of 8 strains of bacteria, under conditions of low and high-ionic strength (1 and 100 mM, respectively) to 11 different surfaces and examined adhesion as a function of charge, hydrophobicity (water contact angle) and surface energy. Inorganic surfaces included three uncoated glass surfaces and eight metal-oxide thin films prepared on the upper (non-tin-exposed) side of float glass by chemical vapor deposition. The Gram-negative bacteria differed in lengths of lipopolysaccharides on their outer surface (three *Escherichia coli* strains), the amounts of exopolysaccharides (two *Pseudomonas aeruginosa* strains), and their known relative adhesion to sand grains (two *Burkholderia cepacia* strains). One Gram positive bacterium was also used that had a lower adhesion to glass than these other bacteria (*Bacillus subtilis*). For all eight bacteria, there was a consistent increase in adhesion between with the type of inorganic surface in the order: float glass exposed to tin (coded here as Si-Sn), glass microscope slide (Si-m), uncoated air-side float glass surface (Si-a), followed by thin films of  $(\text{Co}_{1-y-z}\text{Fe}_y\text{Cr}_z)_3\text{O}_4$ , Ti/Fe/O,  $\text{TiO}_2$ ,  $\text{SnO}_2$ ,  $\text{SnO}_2\text{:F}$ ,  $\text{SnO}_2\text{:Sb}$ ,  $\text{Al}_2\text{O}_3$ , and  $\text{Fe}_2\text{O}_3$  (the colon indicates metal doping, a slash indicates that the metal is a major component, while the dash is used to distinguish surfaces). Increasing the ionic strength from 1 to 100 mM increased adhesion by a factor of  $2.0 \pm 0.6$  (73% of the sample results were within the 95% CI) showing electrostatic charge was important in adhesion. However, adhesion was not significantly correlated with bacterial charge and contact angle. Adhesion ( $A$ ) of the eight strains was significantly ( $P < 10^{-25}$ ) correlated with total adhesion free energy ( $U$ ) between the bacteria and surface ( $A = 2162 e^{-1.8U}$ ). Although the correlation was significant, agreement between the model and data was poor for the low energy surfaces ( $R^2 = 0.68$ ), indicating that better models or additional methods to characterize bacteria and surfaces are still needed to more accurately describe initial bacterial adhesion to inorganic surfaces.

© 2004 Elsevier B.V. All rights reserved.

**Keywords:** Metal oxide; Adhesion; *Escherichia coli*

## 1. Introduction

Bacterial adhesion that leads to biofouling is a widespread problem that affects the functioning of a variety of engineered systems including water distribution pipes [1], water treatment membranes [2,3], boat hull surfaces [4,5], cooling towers [6,7], and bacterial delivery (bioaugmentation) systems for in situ bioremediation [8–12]. Our primary interests are in understanding and controlling bacterial transport in sandy groundwater aquifers. Inorganic surfaces in these systems can be idealized as consisting of quartz particles

containing patchy distributions of metal oxides. Under typical groundwater conditions, the quartz and bacteria are both negatively charged and therefore repel each other. However, the metal oxides provide a positively-charged surface that can significantly increase deposition in proportion to the percentage of  $\text{Fe}_2\text{O}_3$  on the quartz surface [13,14]. Aquifers are more complex than this idealized system, as soils contain many other metals as well as natural organic matter (NOM) making it difficult to predict the extent of bacterial adhesion to surfaces. Dissolved natural organic matter (DOM), for example, adsorbs to iron oxide patches on the quartz surfaces, resulting in bacterial adhesion at levels only slightly larger than quartz alone [15].

In order to better understand the factors that control adhesion in natural and engineered systems, bacteria adhesion

\* Corresponding author. Tel.: +1 717 948 6129; fax: +1 717 948 6580.  
E-mail address: [bxl28@psu.edu](mailto:bxl28@psu.edu) (B. Li).

to surfaces has been analyzed in terms of bacteria and surface hydrophobicity and charge [16–18], surface roughness [19,20], the presence of conditioning films on a surface, or the polymers on bacteria [15,21,22]. The effects of solution chemistry on adhesion, such as pH [23,24] and ionic strength [25,26], have been examined as well. In these studies, changes in adhesion are usually examined for a small number of bacterial strains or types of surfaces. There have been few efforts to produce large adhesion data sets (i.e. for a number of different bacteria and surfaces) needed to test energy-based adhesion models. One data set for a large number of bacteria was developed by van Loosedrecht et al. [27]. They showed that for a hydrophilic (glass) and hydrophobic (sulphated polystyrene disks), the percentage of bacteria attaching to the surface was related to both the hydrophobicity (water contact angle) of the bacterium and its charge (zeta potential). However, they were not able to combine data from the two different surfaces into a single model that could be used to explain and predict bacterial adhesion based on cell and surface properties. Others have analyzed the adhesion of one or two bacteria to surfaces using DLVO theory, a model that accounts for the electrostatic repulsion and van der Waals attractive forces between a colloid and surface, or extended DLVO (XDLVO) theory, which additionally accounts for acid–base interactions [28–31]. XDLVO-based analyses have provided support for the importance of the properties of both the surface and the colloids in adhesion, but the model has not been tested in a single study using a wide range of bacteria and surfaces [32–34].

The effect of metal oxides on adhesion is of particular interest for understanding bacterial adhesion. There are a variety of metal oxides present in soils and many manufactured materials such as tin, titanium and iron oxides are used in industrial processes as well. For example, TiO<sub>2</sub> is vapor-deposited on glass to change the transmission properties of windows [35], and TiO<sub>2</sub> particles are used in a number of manufactured products such as toothpaste and paint [36]. Only a few metal oxides have previously been examined in bioadhesion studies. Most of that work has focused on iron oxides [14,15,37–40] that are known to increase bacterial adhesion. The influence of other metals and metal oxides on bacterial adhesion is not well understood, although there is general agreement that polyvalent cations increase adhesion [18] and that the adsorption of organic matter onto metal oxides (iron and aluminum hydroxides) reduces adhesion by masking positive charges [13,39]. It has been shown that lipopolysaccharide (LPS) on the surface of Gram-negative bacteria contained high-affinity binding sites for bivalent cations [18,40,41], and that the affinity of *Escherichia coli* increased as the molecular mass of the O-antigen of the LPS increased for TiO<sub>2</sub> and Al<sub>2</sub>O<sub>3</sub> surfaces [42].

In this study, the adhesion of 8 bacteria to 11 metal oxide-coated and uncoated glass surfaces was tested to determine the effect of these different inorganic surfaces on bacterial adhesion. The bacteria were chosen based on differences in their outer surfaces. Three strains of *E. coli*

with progressively truncated lipopolysaccharides were chosen based on findings that the length of the LPS molecule was inversely related to adhesion to a hydrophilic surface [43–45], while four additional bacteria were chosen based on production of extracellular polymeric substances (EPS) or large differences in their adhesion to sand. Because these seven bacterial strains were all Gram negative, a Gram positive bacterium (which does not contain LPS) was also included (*Bacillus subtilis*) in the study. We analyzed adhesion data to determine whether existing three different models, based on XDLVO theory, could be used to explain trends in adhesion based on bacteria and surface properties (surface potentials and contact angles).

## 2. Methods

### 2.1. Bacteria

Eight different strains of bacteria were used in these experiments that differ in their surface and adhesive properties. The three *E. coli* K12 strains examined here had distinctly different lipopolysaccharide outer layers [44,45]. LPS in Gram negative bacteria, such as *E. coli*, normally contains three components: keto-deoxy-octulonate (KDO); a core polysaccharide; and a large O-antigen. *E. coli* strain D21 contains the keto-deoxy-octulonate and inner and outer core polysaccharide but no O-antigen, while a mutant of this strain (*E. coli* D21f2) has only the KDO. *E. coli* K-12 strain JM109 has a complete LPS layer. Two *Burkholderia cepacia* strains used in this study were selected due to large differences in adhesion properties: the parent strain G4, and its non-adhesive mutant, Env435 [46]. *B. cepacia* G4 is an environmentally relevant bacterium capable of degrading trichloroethylene (TCE), polychlorinated biphenyls (PCBs), benzene and toluene [47–50]. Two strains of *Pseudomonas aeruginosa* were chosen for their differing production of extracellular polymeric substances: the wild type PA01 produces a normal amount of EPS, while the mucoid mutant PDO300 is an overproducer of EPS [51–53]. *P. aeruginosa* has been extensively used to study initial biofilm formation and bioremediation [54–57]. *P. aeruginosa* is an opportunistic pathogen routinely found in bacterial infestations in humans in immune-compromised individuals and in contaminated human implants. *B. subtilis* (ATCC 7003) was used as a representative, well studied, Gram positive bacterium. Gram positive bacteria do not contain LPS on their outer membrane, and have a thick external layer of peptidoglycan.

*E. coli* strains D21 and D21f2 were obtained from the *E. coli* Genetic Stock Center and Yale University, and strain JM109 was obtained from Shahriar Mobashery at Wayne State University. The two *B. cepacia* strains were obtained from Mary DeFlaun at Envirogen Corp. *P. aeruginosa* strains were provided by Matt Parsek at Northwestern University. *B. subtilis* was obtained from Jon Chorover at The University of Arizona.

Bacteria were grown in Luria broth Millers at 26 °C and harvested during mid-log-growth at a cell concentration of  $\sim 10^8$  ml<sup>-1</sup>. The harvested bacteria were washed three times in phosphate buffer solutions (PBS) at a pH of 7.1–7.3, at one of two different ionic strengths: 100 mM (0.29 g KH<sub>2</sub>PO<sub>4</sub>, 1.56 g K<sub>2</sub>HPO<sub>4</sub>·3H<sub>2</sub>O, 4.93 g NaCl in 1 L water) (PBS-100); or 1 mM (0.026 g KH<sub>2</sub>PO<sub>4</sub>, 0.047 g K<sub>2</sub>HPO<sub>4</sub> in 1 L water) (PBS-1). Cells were resuspended in PBS for adhesion experiments to an optical density at 600 nm of  $-0.5$ , with cell concentrations in the range of  $4\text{--}6 \times 10^7$  mL<sup>-1</sup> based on acridine orange direct counts (AODC) [58].

## 2.2. Glass

The 11 different glass and metal oxide-coated glass surfaces used in this study are designated in this study as follows: Si-m, Si-a, Si-Sn, TiO<sub>2</sub>, SnO<sub>2</sub>, Al<sub>2</sub>O<sub>3</sub>, Fe<sub>2</sub>O<sub>3</sub>, Co/Fe/Cr/O, SnO<sub>2</sub>:Sb, SnO<sub>2</sub>:F, and Ti/Fe/O (the colon indicates metal doping, a slash that the metal is a major component, while the dash is used to distinguish surfaces). A typical borosilicate glass microscope slide (designated as Si-m) was used for all experiments as these slides are widely available (Corning Microslide, Cat. no. 2948, glass no. 0215). Two other two glass surfaces were: the bottom of the glass exposed to molten tin during the float glass production (Si-Sn), and the upper (uncoated) glass surface exposed to the air during production (Sn-a). Electron microprobe studies have demonstrated that exposure of the glass to molten tin results in a 2% (by weight) concentration of tin oxide [59]. The glass samples coated with metal-oxide films were provided by C. Steffek, PPG Industries Inc. The 20–500 nm-thick films were produced by different previously described vapor deposition techniques [60–63]. Four of the surfaces are metal oxides with known stoichiometry (TiO<sub>2</sub>, SnO<sub>2</sub>, Al<sub>2</sub>O<sub>3</sub>, Fe<sub>2</sub>O<sub>3</sub>). The metals in the surface designated as Co/Fe/Cr/O has a known stoichiometry of (Co<sub>1-y-z</sub>Fe<sub>y</sub>Cr<sub>z</sub>)<sub>3</sub>O<sub>4</sub> while the other metal-oxide surfaces (SnO<sub>2</sub>:Sb, SnO<sub>2</sub>:F, and Ti/Fe/O) are mixtures of the metals. SnO<sub>2</sub>:Sb contains 8% Sb, SnO<sub>2</sub>:F contains 3% F, and Ti/Fe/O is a 50:50 mixture of the two metal oxides.

Each glass surface (2.5 cm × 7.6 cm) was cleaned (0.2% (v/v) Dart210 cleaning solution, Madison Chemical Company, pH 2.9) in a sonicator at 60 °C for 20 min, and then at 40 °C for 10 min, and then rinsed with deionized water and dried with nitrogen gas [64].

## 2.3. Bioadhesion tests

Various techniques have been developed to evaluate initial bacterial adhesion, including: surfaces exposed to solutions under various mixed fluid conditions [37], flat plates in laminar flow fields [65], and columns packed with various types of particles [13,18,48,66]. In some cases, a surface was immersed in a solution that was mixed (shaken) during exposure [37], while in others, the solution was placed as a drop on the surface and then the surface was rinsed off [27].

In order to evaluate adhesion for a large number of bacteria and glass surfaces, we developed an adhesion procedure based on exposure of a fixed concentration of bacteria to a surface for a fixed time, which we refer to as the microbial adhesion to glass (MAG) test. In the MAG test, all experimental variables except the bacterial strain or surface type were held constant, including cell concentration, exposure time, shaking speed, container size and solution volume.

Bacteria used in the MAG test were washed and resuspended in PBS solution (PBS-1 or PBS-100) in centrifuge tubes (50 mL) containing a single surface (2.5 cm × 7.6 cm). Tubes were shaken at 26 °C for 2 h, the glass was removed and rinsed three times with PBS solution (25 ml), and then cells were enumerated (10 fields) by acridine orange direct counts (58) using a fluorescence microscope (Olympus BH2).

## 2.4. Contact angle

Contact angle measurements were performed in triplicate using a goniometer (Newport Optical Inc.) by the sessile drop method [67,68]. One drop of a liquid (3 μl) was deposited onto a dry glass surface or a lawn of bacteria. Images of drops were magnified, photographed, and the contact angle measured using an image analysis program (Scion Beta 4.02 for windows, Scioncorp, Frederick, MD). Lawns of bacteria were prepared by filtering 10–20 mL of a cell suspension (10<sup>8</sup>/mL, harvested in mid-log-growth phase), prepared as described above, onto an aluminum oxide filter (Anodisc, 0.2 μm pore size, 25 mm diameter; Whatman Corp.). Each filter, containing approximately 70 layers of bacteria, was rinsed with 5 mL of deionized water. Lawns were dried in a Petri dish for at least 1 h and measured within 30 min. Previous studies have shown that after a drying time of 30 min, measurements on lawns are stable for several hours [69–72]. Contact angles were measured within 2 s for 4 μL droplets (triplicate samples) of one non-polar (diiodomethane) and two polar (glycerol and deionized water) solutions [67].

## 2.5. Surface charge

Zeta potentials of bacteria, assumed to be equal to the cell surface charge [73,74], were calculated from electrophoretic mobilities. Cells prepared as described above were resuspended in 1 or 100 mM PBS solutions, and zeta potentials measured five times (triplicate samples) using 20 cycles per analysis (ZetaPALS analyzer, Brookhaven Instruments Corp.). Glass and metal-oxide surface charge was determined using an asymmetric clamping cell (Anton Paar, Graz, Austria) connected with a commercial streaming potential analyzer (EKA, Brookhaven Instruments, Holtsville, NY) according to methods described in Walkson et al. [75]. Surface charge is reported here only for the 1 mM solution (25 °C, pH 7.3–7.5) as measurements obtained with the 100 mM solution produced erratic and inconsistent values.

## 2.6. Surface roughness measurements

The roughness of glass and metal-oxide surfaces was measured using an atomic force microscope (AFM; Bioscope, Digital Instruments) consisting of an AFM head mounted on an inverted microscope. Glass surface roughness was measured using contact mode in air with DNP-S silicon nitride cantilevers (Digital Instrument) having a force constant of 0.045 N/m (the long/thin tip) as measured by the Cleveland method [76]. All tips were cleaned in a Bioforce UV/ozone cleaner before use. Height images were used to calculate the roughness measurement based on root mean square (RMS) values.

## 2.7. Model

The total energy  $U_{\text{swb}}$  (J) needed to bring a bacterium (b) from an infinite distance to a surface (s) in water (w) was calculated using XDLVO theory, as:

$$U_{\text{swb}} = U_{\text{swb}}^{\text{LW}} + U_{\text{swb}}^{\text{AB}} + U_{\text{swb}}^{\text{EL}} \quad (1)$$

where the superscripts indicate interactions due to Lifshitz–van der Waals (LW), electrostatic (EL), or the acid–base (AB) forces arising from hydrogen bonding between two surfaces immersed in a polar solvent (e.g. water) [67,68,77,78].  $U^{\text{LW}}$  was calculated using the retarded Hamaker expression [79–82]. The individual components of the total energy [77,78,82,83] are:

$$U_{\text{swb}}^{\text{LW}} = \frac{-Ha}{6h(1 + 14h/\lambda)} \quad (2)$$

$$U_{\text{swb}}^{\text{AB}} = 2\pi a\lambda_1 \Delta G_{h_0}^{\text{AB}} \exp\left(\frac{h_0 - h}{\lambda_1}\right) \quad (3)$$

$$U_{\text{swb}}^{\text{EL}} = \pi\epsilon a \left[ 2\Psi_b\Psi_s \ln\left(\frac{1 + e^{-\kappa h}}{1 - e^{-\kappa h}}\right) + (\Psi_b^2 + \Psi_s^2) \ln(1 - e^{-2\kappa h}) \right] \quad (4)$$

$H$  (J) is the Hamaker constant calculated as  $H = -12\pi h_0^2 \Delta G_{h_0}^{\text{LW}}$  [84],  $a$  (m) the bacterial radius and  $\lambda$  the characteristic wavelength of the interaction (assumed to be 100 nm according to 80),  $\epsilon = 80 \times 8.854 \times 10^{-12}$  ( $\text{C}^2 \text{J}^{-1} \text{m}^{-1}$ ) is the permittivity of water,  $\Psi$  (mV) the surface potential, and  $\kappa$  ( $\text{m}^{-1}$ ) the inverse Debye length calculated as  $\kappa = 0.304 M^{-1/2}$  where  $M$  [M] is the ionic strength. The characteristic decay of acid–base interactions in water,  $\lambda_1$  ranges between 0.2 and 1.0 nm, and is defined here as 0.6 nm as in previous studies [83]. The minimum separation distance between the bacterium and surface,  $h_0$ , is usually defined as 0.158 nm, and may be regarded as the distance between the outer electron shells (van der Waals boundaries) of adjoining non-covalently interacting molecules [78,83]. The surface potential was assumed to be same as

the measured zeta potentials for the surfaces, either using electrophoretic mobility (bacteria) or streaming potential (glass and metal-oxide surfaces) [68]. Energy ( $U_{\text{swb}}$ ) was calculated on the basis of moving a bacterium to within  $h = 5$  nm of a surface, roughly equal to the length of the core polysaccharide of Gram negative bacteria [85].

The interaction energy per unit area between the bacterium (b) and a surface (s),  $\Delta G_{h_0}$  ( $\text{mJ}/\text{m}^2$ ), at the minimum separation distance  $h_0$ , is calculated as for Lifshitz–van der Waals and acid–base interactions [67,68,77] using:

$$\Delta G_{h_0}^{\text{LW}} = 2 \left( \sqrt{\gamma_w^{\text{LW}}} - \sqrt{\gamma_s^{\text{LW}}} \right) \left( \sqrt{\gamma_b^{\text{LW}}} - \sqrt{\gamma_w^{\text{LW}}} \right) \quad (5)$$

$$\begin{aligned} \Delta G_{h_0}^{\text{AB}} = & 2\sqrt{\gamma_w^+} \left( \sqrt{\gamma_s^-} + \sqrt{\gamma_b^-} - \sqrt{\gamma_w^-} \right) \\ & + 2\sqrt{\gamma_w^-} \left( \sqrt{\gamma_s^+} + \sqrt{\gamma_b^+} - \sqrt{\gamma_w^+} \right) \\ & - 2 \left( \sqrt{\gamma_s^+ \gamma_b^-} + \sqrt{\gamma_b^+ \gamma_s^-} \right) \end{aligned} \quad (6)$$

where + indicates the electron acceptor and – the electron donor.

According to van Oss [71,72,78,86], the total surface energy of a pure substance is the defined as the sum of the surface tensions due to the LW and AB components, or

$$\gamma^{\text{total}} = \gamma^{\text{LW}} + \gamma^{\text{AB}} \quad (7)$$

where  $\gamma^{\text{AB}} = 2\sqrt{\gamma^+ \gamma^-}$ . Using the extended Young equation, or

$$(1 + \cos \theta_{ij}) \gamma_j^{\text{total}} = 2 \left( \sqrt{\gamma_i^{\text{LW}} \gamma_j^{\text{LW}}} + \sqrt{\gamma_i^+ \gamma_j^-} + \sqrt{\gamma_i^- \gamma_j^+} \right) \quad (8)$$

the measured contact angles  $\theta_{ij}$  of three probe solutions on a surface can be used to determine the surface tension parameters of the surface and liquid [68]. The surface tensions of the three solutions,  $\gamma_j$  ( $\text{mJ}/\text{m}^2$ ; where  $j$  is w = water, g = glycerol, or m = diiodomethane) are known constants [67,68]. The apolar liquid (diiodomethane) was first used to calculate the non-polar surface tension,  $\gamma_i^{\text{LW}}$ , as  $\gamma_m^+ = \gamma_m^- = 0$ . Using Eq. (8) for water and glycerol, we then obtained  $\gamma_i^+$  and  $\gamma_i^-$ .

## 3. Results

### 3.1. Bacteria properties

Two of the *E. coli* strains (D21 and JM109) were hydrophilic, as they had water contact angles less than 25 °C [34,68] (Table 1). All of the other strains were hydrophobic with water contact angles ranging from 30 to 39 °C. All bacteria were negatively charged, with zeta potentials ranging from –20 to –53 mV in a 1 mM solution (PBS-1)

Table 1  
Contact angles of bacteria and glass surfaces

Surface	Contact angle (degrees)		
	Water	Glycerol	Diiodomethane
<i>E. coli</i> JM109	19 ± 2	40 ± 4	43 ± 2
<i>E. coli</i> D21	19 ± 4	27 ± 3	40 ± 3
<i>E. coli</i> D2	39 ± 6	75 ± 3	40 ± 3
<i>B. cepacia</i> G4	37 ± 4	62 ± 2	48 ± 5
<i>B. cepacia</i> Env435	30 ± 3	62 ± 2	50 ± 4
<i>P. aeruginosa</i> PA01	35 ± 4	57 ± 3	36 ± 4
<i>P. aeruginosa</i> PDO300	30 ± 3	50 ± 4	32 ± 2
<i>B. subtilis</i> 7003	33 ± 2	45 ± 2	66 ± 2
Si–Sn	9 ± 2	19 ± 2	34 ± 2
Si-m	13 ± 3	17 ± 4	25 ± 2
Si-a	22 ± 3	21 ± 2	34 ± 4
Co/Fe/Cr/O	62 ± 4	69 ± 4	35 ± 2
Ti/Fe/O	52 ± 4	58 ± 2	21 ± 2
TiO <sub>2</sub>	59 ± 2	55 ± 4	27 ± 3
SnO <sub>2</sub>	60 ± 3	59 ± 2	32 ± 2
SnO <sub>2</sub> :Sb	45 ± 7	50 ± 3	23 ± 4
SnO <sub>2</sub> :F	57 ± 2	46 ± 3	20 ± 2
Al <sub>2</sub> O <sub>3</sub>	62 ± 5	48 ± 2	23 ± 2
Fe <sub>2</sub> O <sub>3</sub>	68 ± 5	57 ± 3	24 ± 3

(Table 2). Bacteria zeta potentials decreased in the 100 mM solution (range of  $-8$  to  $-40$  mV) by 25–47%, except for *P. aeruginosa* which decreased by 75% solution. There was no significant correlation between water contact angle and zeta potential for the eight strains of bacteria ( $R^2 = 0.07$ ,  $P = 0.52$ ). The equivalent spherical radius of the bacteria ranged from  $0.37 \mu\text{m}$  for *B. cepacia* G4 to  $1.12 \mu\text{m}$  for *B. subtilis*, with no differences in cell size in the two different two ionic strength solutions.

### 3.2. Glass and metal-oxide properties

The side of the glass exposed to molten tin during manufacture (designated as Si–Sn) produced the most hydrophilic surface (contact angle:  $9 \pm 2^\circ$ , Table 1) among the glass and metal-oxide surfaces. Two other surfaces, the uncoated glass surface (Si-a) and the microscope slide (Si-m), had water contact angles less than  $25^\circ$  and were therefore hydrophilic. All metal-oxide surfaces were hydrophobic, with contact angles ranging from  $45^\circ$  (SnO<sub>2</sub>:Sb) to  $68^\circ$  (Fe<sub>2</sub>O<sub>3</sub>). All the

Table 2  
Bacteria size (equivalent radius) and zeta potentials

Bacteria	Radius ( $\mu\text{m}$ )	Zeta potential (mV) (1 mM)	Zeta potential (mV) (100 mM)
<i>E. coli</i> JM109	$0.65 \pm 0.12$	$-53 \pm 5$	$-32 \pm 6$
<i>E. coli</i> D21	$0.59 \pm 0.14$	$-50 \pm 5$	$-34 \pm 6$
<i>E. coli</i> D21f2	$0.61 \pm 0.14$	$-57 \pm 6$	$-40 \pm 6$
<i>B. cepacia</i> G4	$0.37 \pm 0.08$	$-20 \pm 2$	$-11 \pm 4$
<i>B. cepacia</i> Env 435	$0.40 \pm 0.07$	$-27 \pm 3$	$-21 \pm 3$
<i>P. aeruginosa</i> PA01	$0.51 \pm 0.13$	$-40 \pm 3$	$-21 \pm 2$
<i>P. aeruginosa</i> PDO300	$0.50 \pm 0.17$	$-32 \pm 3$	$-8 \pm 1$
<i>B. subtilis</i> 7003	$1.12 \pm 0.20$	$-39 \pm 6$	$-26 \pm 2$

Table 3  
Glass and metal-oxide surface roughness and surface charge (IS = 1 mM)

Glass	Roughness (nm)	Surface charge (mV)
Si–Sn	$4.3 \pm 0.8$	$-56.3 \pm 0.6$
Si-m	$6.2 \pm 0.6$	$-36.5 \pm 0.5$
Si-a	$4.1 \pm 0.7$	$-9.3 \pm 0.4$
SnO <sub>2</sub> :Sb	$16.0 \pm 2.1$	$-26.7 \pm 0.6$
Ti/Fe/O	$5.2 \pm 0.5$	$-31.9 \pm 0.4$
SnO <sub>2</sub> :F	$17.6 \pm 1.8$	$-30.5 \pm 0.7$
TiO <sub>2</sub>	$9.4 \pm 1.2$	$-39.3 \pm 0.2$
SnO <sub>2</sub>	$6.5 \pm 0.6$	$-28.2 \pm 0.3$
Al <sub>2</sub> O <sub>3</sub>	$4.8 \pm 0.8$	$-26.2 \pm 0.5$
Co/Fe/Cr/O	$8.1 \pm 1.1$	$-50.2 \pm 0.9$
Fe <sub>2</sub> O <sub>3</sub>	$6.5 \pm 0.7$	$-30.1 \pm 0.4$

glass and metal-oxide surfaces were negatively charged in the 1 mM ionic strength solution, with surface charges ranging from  $-56.3 \pm 0.6$  mV for Si–Sn, to  $-9.3 \pm 0.4$  mV for Si-a glass. There was no significant correlation between water contact angle and glass surface charge ( $R^2 = 0.01$ ,  $P = 0.74$ ). Nine of the surfaces had an average roughness of less than 10 nm (range 4.1–9.4 nm; Table 3). Two of the metal-oxide surfaces had higher average roughness values of  $16 \pm 2.1$  nm (SnO<sub>2</sub>:Sb) and  $17.4 \pm 1.8$  nm (SnO<sub>2</sub>:F). These two surfaces also had much thicker metal-oxide coatings (500 nm) than the other vapor-deposited metal-oxide surfaces (between 25 and 60 nm) [60–62].

### 3.3. Adhesion of bacteria to surfaces

The order of increasing adhesion of the eight strains of bacteria was consistent for the 11 different glass and metal-oxide surfaces. In 1 mM PBS solution, all eight strains of bacteria adhered the least to Si–Sn glass ( $<1600 \text{ mm}^{-2}$ , Fig. 1A), followed by the other two hydrophilic glass surfaces (Si-m and Si-a). Bacterial adhesion was greatest to the Fe<sub>2</sub>O<sub>3</sub>-coated glass, which was also the most hydrophobic surface.

The extent of adhesion varied among the different bacteria in a manner generally consistent with our expectations regarding the influence of lipopolysaccharide length and presence or absence of large amounts of extracellular polymeric substances. The three *E. coli* strains with LPS lengths that increased in the order D21f2, D21, and JM109, increased in adhesion values for each of the 11 surfaces. This increase in adhesion with LPS length is consistent with previous adhesion results obtained for these three *E. coli* strains in column tests using glass beads in a low ionic strength solution; however, at a higher ionic strength there was no correlation found between adhesion and LPS length [45]. Both *Pseudomonas* strains, known to produce large amounts of EPS, had the highest numbers of cells attached among the 8 strains for each of the 11 surfaces. *P. aeruginosa* PDO300, an over-producer of EPS, adhered the most, followed by the wild type (*P. aeruginosa* PA01), which produced lesser amounts of EPS. *B. cepacia* G4 adhered more than its non-adhesive

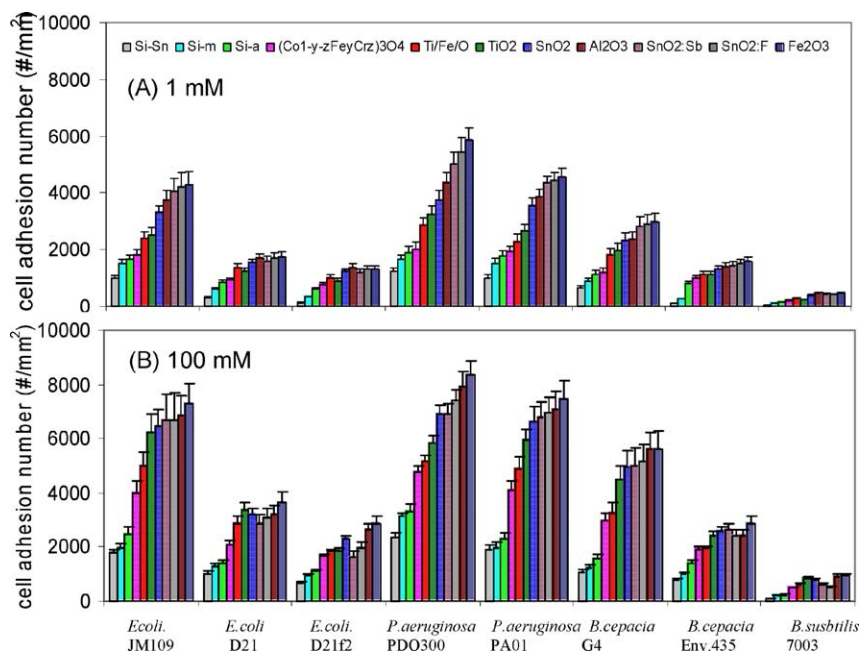


Fig. 1. The adhesion of eight strains of bacteria on 11 glass and metal-oxide surfaces in (A) 1 and (B) 100 mM solutions. The order of the results shown in the bar plots is the same as that given by the legend. Error bars are  $\pm$ S.D.

mutant Env435. *B. subtilis* 7003, which lacks LPS, adhered the least of the eight bacterial strains to the different surfaces despite having the highest water contact angle ( $33^\circ$ ) of the different bacterial strains.

### 3.4. Effect of ionic strength on bacterial adhesion

The same trends in adhesion observed between bacteria and surfaces at low ionic strength (1 mM) were also observed at the higher ionic strength (100 mM): in general, the most hydrophilic surfaces had the fewest number of bacteria adhered, while the hydrophobic surfaces had larger numbers of attached bacteria (Fig. 1B). Increasing the ionic strength from 1 to 100 mM produced a nearly consistent increase of  $2.0 \pm 0.6$  ( $\pm$ S.D.; range 1.2–4.0). This increase in adhesion with ionic strength is consistent with other research showing adhesion in proportion to ionic strength [26,87,88].

### 3.5. Adhesion analyzed in terms of bacteria/glass surface contact angle and zeta potential

Previous research has shown that when there is a large difference in the water contact angle of two surfaces, bacterial adhesion can be explained on the basis of the zeta potential and water contact angle of the bacteria [27]. We therefore examined adhesion data for the two surfaces with the greatest differences in their water contact angles (Si–Sn glass and  $\text{Fe}_2\text{O}_3$ -coated glass) solely on the basis of bacterial zeta potential and water contact angle. Bacterial adhesion was observed to be negatively correlated with bacterial zeta potential for both surfaces, as expected based on previous results [27] (Fig. 2). However, in both cases adhe-

sion was inversely correlated with water contact angle. This latter result contradicted previous findings [27] of increasing adhesion with bacterial water contact angle. Bacterial adhesion was not significantly correlated with bacterial surface water contact angle (linear correlation,  $Y = -88.3X + 5102$ ,  $P < 0.35$ ,  $R^2 = 0.22$ ; non-linear correlation of form  $Y = 5963 e^{-0.035X}$ ,  $P < 0.46$ ,  $R^2 = 0.16$ ) or surface charge (linear correlation,  $Y = -4.45X + 2419$ ,  $P < 0.94$ ,  $R^2 = 0.002$ ; non-linear correlation of form  $Y = 2065 e^{-0.001X}$ ,  $P < 0.90$ ,  $R^2 = 0.0003$ ). As for glass surface properties, the bacterial adhesion was not correlated with glass surface charge (linear correlation,  $Y = 24.63X + 3420$ ,  $P < 0.38$ ,  $R^2 = 0.09$ ; non-linear correlation of form of  $Y = 3627 e^{0.0131X}$ ,  $P < 0.34$ ,  $R^2 = 0.10$ ), but was significantly correlated

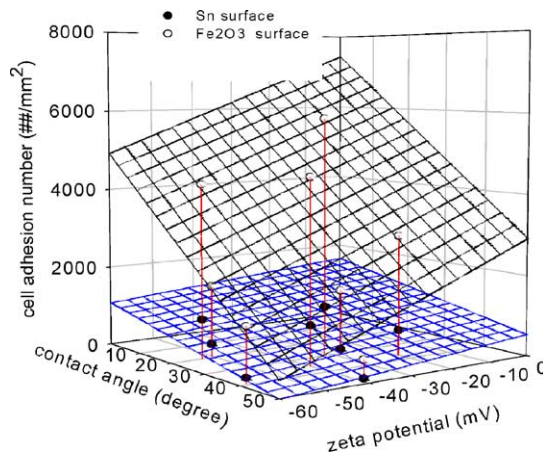


Fig. 2. Bacterial adhesion to a hydrophobic ( $\text{Fe}_2\text{O}_3$ ) and hydrophilic (Si–Sn) surface based on bacterial zeta potential and water contact angle.

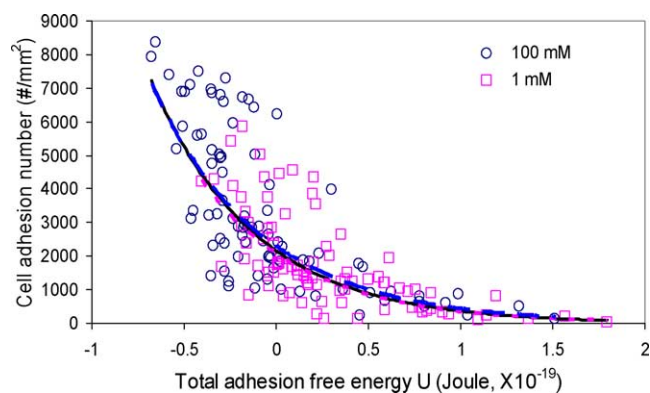


Fig. 3. Bacterial adhesion correlated with total adhesion free energy ( $U$ ) in: 1 mM ( $A = 2060 e^{-1.8U}$ ,  $R^2 = 0.60$ ,  $P < 10^{-13}$ ), 100 mM ( $A = 2155 e^{-1.9U}$ ,  $R^2 = 0.67$ ,  $P < 10^{-13}$ ), and both 1 and 100 mM ( $A = 2123 e^{-1.9U}$ ,  $R^2 = 0.67$ ,  $P < 10^{-26}$ ) ionic strength solutions.

with glass surface water contact angle (linear correlation,  $Y = 44.70X + 534.1$ ,  $P < 10^{-4}$ ,  $R^2 = 0.81$ ; non-linear correlation of form of  $Y = 826 e^{0.023X}$ ,  $P < 10^{-5}$ ,  $R^2 = 0.87$ ). This suggested that the substratum hydrophobicity played an important role in determining bacterial adhesion.

### 3.6. Analysis of adhesion data using a model based on surface energy

Adhesion (at both ionic strengths) and free energy were significantly correlated ( $A = 2123 e^{-1.9U}$ ;  $P < 10^{-26}$ ,  $R^2 = 0.68$ ) (Fig. 3). Correlations based on data from only one ionic strength (1 or 100 mM) were similarly significant. The distance used in the analysis of the total energy needed to bring the bacterium to within 5 nm of the surface was not critical to our conclusion as correlations developed at other distances (2–20 nm) were similarly significant. The wide variation in the data at the lowest surface energies indicates that not all bacterial-surface adhesion events were well explained. Using the regression model, we compared the measured and predicted energies grouped according to bacterium. The predicted values (Fig. 4) did not match well

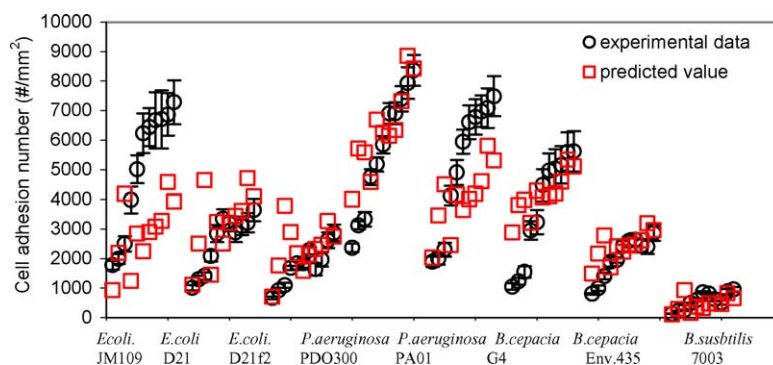


Fig. 4. Adhesion measured in experiments compared with model predictions ( $A = 2155 e^{-1.9U}$ ; 100 mM solution) for the 11 surfaces arranged by the specific bacterial strain.

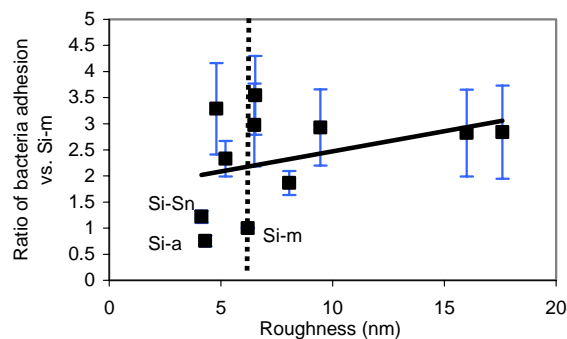


Fig. 5. Bacterial adhesion, normalized to the value obtained for the Si-m glass surface, as a function of surface roughness. The regression line shown is not significant ( $R^2 = 0.14$ ,  $P < 0.26$ ). Error bars represent the range of adhesion values.

with experimental values primarily for two strains, *E. coli* JM109 and *P. aeruginosa* PA01.

### 3.7. Effect of nanoscale surface roughness on bacterial adhesion

Surface roughness is not included in XDLVO theory but it may also impact bacterial adhesion [20,68]. Glass and metal-oxide surface roughness varied among the samples (Table 3, with the two roughest surfaces being the SnO<sub>2</sub>:F and SnO<sub>2</sub>:Sb-coated surfaces. In order to compare the relative effect of roughness, we normalized the average surface roughness values for each surface to that of the Si-m (glass slide) surface. There was no significant ( $P = 0.26$ ) effect of surface roughness on bacterial adhesion (Fig. 5). However, we note two potential trends. First, adhesion was always larger to the surfaces that were rougher than the glass slide (surface roughness larger than unity). Second, there was relatively little variation among the adhesion of the eight strains of bacteria to the two smoothest surfaces (Si-Sn and Si-a). Thus, there may be ranges of surface roughness over which adhesion is not correlated with roughness.

#### 4. Discussion

Metal-oxide coatings consistently increased bacterial adhesion compared to uncoated glass surfaces (Si-a and Si-m) or the side of the float glass exposed tin during glass production (Si-Sn). One noticeable change in the surface produced by the metal-oxide coating was increased hydrophobicity. The two uncoated glass surfaces (Si-a and Si-m) and the Sn-exposed surface (Si-Sn) were hydrophilic, with water contact angles of 9 and 22°, while the metal-oxide surfaces were all hydrophobic, with water contact angles of 45–68°. In contrast, the surface charge of the surfaces appeared to have a less direct influence on bacterial adhesion. The three surfaces with the lowest numbers of bacterial adhesion (for each of the eight bacterial strains) had the largest range of surface potentials (−9 to −56 mV).

There was always a consistent order of increasing bacterial adhesion to the 11 surfaces of: Si-Sn, Si-m, Si-a, Co/Fe/Cr/O, Ti/Fe/O, TiO<sub>2</sub>, SnO<sub>2</sub>, SnO<sub>2</sub>:F, SnO<sub>2</sub>:Sb, Al<sub>2</sub>O<sub>3</sub>, and Fe<sub>2</sub>O<sub>3</sub>. There is evidence that this order was influenced by the presence of the type of metal oxide. For example, the three Sn-oxide surfaces exhibited similar adhesion levels. Fewer bacteria adhered to the glass surface exposed to molten Sn during the manufacturing of the float glass (Fig. 1). Iron oxide produced surfaces within the lower to intermediate ranges of cell adhesion when mixed in with other metals (Co/Fe/Cr/O or Ti/Fe/O), but a pure Fe-oxide coating produced the highest adhesion values.

Surface roughness was probably a factor in adhesion, as all the metal-oxide-coated surfaces had greater bacterial adhesion to their surfaces and were also rougher than uncoated surfaces (Si-a, Si-m and Si-Sn). However, the contribution of roughness was not easily separated from hydrophobicity as all metal oxides were also more hydrophobic than uncoated surfaces. Nano-scale roughness was not designed to be systematically varied in these studies, and thus it was not possible to independently evaluate its contribution to adhesion here. A previous study demonstrated that increasing the nano-scale roughness of a surface from 15 to 38 nm increased colloid and bacterial adhesion in tests based on flow through porous media (silica beads) [20]. In the present study, two surfaces (SnO<sub>2</sub>:F and SnO<sub>2</sub>:Sb) had relatively high-surface roughness values of 16.0 and 17.5 nm, while the other surfaces had an average roughness values ranging from 4.1 to 9.4 nm. The two relatively rough surfaces were at the highest range of measured cell adhesion, with only the iron oxide surface demonstrating greater adhesion by the bacteria in our tests. It has been shown that roughness lowers surface energy, so that electrostatic repulsion and van der Waals attractive forces are considerably lower at rough surfaces than they are for corresponding smooth surfaces [66]. However, we did not find that the surface energy of a rough surface was lower than smooth glass when the two surfaces had similar hydrophobicities. Thus, surface roughness appears to be a contributor to adhesion, but in a manner that was not always as important as the presence of

specific metal oxides (i.e. Fe<sub>2</sub>O<sub>3</sub>) in determining adhesion in the present analysis.

##### 4.1. Contribution of bacterial surface properties to adhesion

It is clear that the polymers on the outer surface of the bacterium affected adhesion, but it is not clear how these differences can be incorporated into predictive models. The adhesion of the three *E. coli* strains increased with the length of the LPS for each strain, and for the two *P. aeruginosa* strains we found that there was greater adhesion of the EPS overproducer (strain PDO300) than the parent strain (PA01). It has been reported that LPS/EPS molecules produce steric repulsion between bacteria and substrate surfaces [18] due to the hydrophilic nature of the biopolymers and the fact that they can generate osmotic forces when they come together [89,90]. Such repulsion between bacteria and surfaces was not observed to occur here because adhesion increased as polymer length increased: *E. coli* JM109 adhesion (complete LPS layer) was larger than adhesion by *E. coli* D21f2 (truncated LPS chain), and the adhesion of the EPS overproducer strain (*P. aeruginosa* PDO300) was larger than normal strain (PA01). Nano-scale measurements of bacterial properties, made using atomic force microscopy measurements, may provide more quantitative predictors of microbial adhesion based on steric interactions. While there are advances being made in this area [34,43,44], however, it is clear that additional work needs to be done to more fully understand the roles of polymers in adhesion [42,91].

##### 4.2. Predicting bacterial adhesion based on surface properties

For a single surface, two bacterial surface properties (water contact angle or surface energy, and zeta potential) were sufficient to predict general trends in differences in adhesion among the bacteria (Fig. 2). Moreover, once an order of bacterial adhesion was established for the eight strains for one surface, the same order of increasing adhesion appeared to occur for the bacteria to any other surface. For example, bacterial adhesion to the Si-m surface increased in the order: *B. subtilis* 7003, *B. cepacia* Env435, *E. coli* D21f2, *E. coli* D21, *B. cepacia* G4, *E. coli* JM109, *P. aeruginosa* PA01, *P. aeruginosa* PDO300. For the Fe<sub>2</sub>O<sub>3</sub> surface, we observed the same order. However, the magnitude of the change in adhesion between the surfaces was not the same. For example, *E. coli* strain D21 adhesion increased by a factor of 9.8 between Si-m and Fe<sub>2</sub>O<sub>3</sub>, while *P. aeruginosa* sp. PDO300 adhesion changed by a factor of 4.2.

Other researchers have concluded that electrostatic interaction between the bacterium and surface is the main factor affecting bacterial adhesion, with hydrophobic interactions and polymer bridging playing only minor roles [29,40]. Their conclusions were based on bacterial adsorption in solutions of different ionic strength, however, and

not on different surfaces at a single ionic strength. We observed a much greater correlation of adhesion with surface energy (based on three liquid contact angles) than surface charge for the different surfaces at a fixed ionic strength. It must be recognized that a decrease in the ionic strength not only decreases surface charge, but it also changes the lengths and conformations of polymers on a bacterial surface [34]. When the ionic strength was increased from 1 to 100 mM, the zeta potential changed by a factor of 0.3 (1/3.33) to 0.5 (1/2), or an average of a factor of  $0.40 \pm 0.16$ . This change was well correlated to the change in adhesion by a factor of  $2.0 \pm 0.6$  between the two ionic strengths. Therefore, it is clear that solution ionic strength played a role in bacterial adhesion. However, the overall change in adhesion produced by ionic strength (a factor of 2.0) is smaller than differences by a factor of 4.2 (*P. aeruginosa* sp. PDO300) and 9.8 (*E. coli* D21) observed between two surfaces (Si-m and Fe<sub>2</sub>O<sub>3</sub>). Thus, while ionic strength appears to correlate well with electrostatic charge for any specific bacterium-surface condition, surface energy was a much better predictor of adhesion to different surfaces.

## Acknowledgements

This study was funded by PPG Industries Inc. and the National Science Foundation (NFS) CRAEMS program (CHE-0089156). The AFM used in this research was partially supported by the Penn State Biogeochemical Research Initiative for Education (BRIE) (NSF IGERT grant DGE-9972759). The authors thank C.B. Greenberg for suggesting the matrix of surfaces used in the study, and M. Elimelech and S. Walker (Yale University) for conducting and analyzing surface charges of the glass and metal-oxide surfaces.

## References

- [1] J.T. Walkers, C.W. Keevil, *Int. Biodeter. Biodegrad.* 34 (1991) 223.
- [2] J. Cho, G. Amy, J. Pellegrino, *Water Res.* 33 (1999) 2517.
- [3] M.K. Korbutowicz, K.M. Nowak, T. Winnicki, *Desalination* 126 (1999) 179.
- [4] K.C. Marshall, R. Stout, R. Mitchell, *Can. J. Microbiol.* 17 (1971) 1413.
- [5] M.J. Dempsey, *Mar. Biol.* 61 (1981) 305.
- [6] J.O.J. Tobin, R.A. Swann, C.L.R. Bartlett, *Br. Med. J.* 282 (1981) 515.
- [7] R.H. Bentham, *Int. Biodeter. Biodegrad.* 31 (1993) 55.
- [8] H.J. Marlow, K.L. Duston, M.R. Wiesner, M.T. Thompson, J.T. Wilson, C.H. Ward, *J. Hazard. Mater.* 28 (1991) 65.
- [9] R.W. Harvey, S.P. Garabedian, *Environ. Sci. Technol.* 25 (1991) 178.
- [10] R.G. Steffan, K.L. Sperry, M.T. Walsh, S. Vainber, C.W. Condee, *Environ. Sci. Technol.* 33 (1999) 2771.
- [11] D.R. Champ, J. Schroeter, *Water Sci. Technol.* 20 (1988) 81.
- [12] L. Jang, P.W. Chang, J.E. Findley, T.F. Yen, *Appl. Environ. Microbiol.* 46 (1983) 1066–1072.
- [13] W.P. Johnson, M.J. Martin, M.J. Gross, B.E. Logan, *Colloid Surf.* 17 (1996) 263.
- [14] J.N. Ryan, M. Elimelech, R.A. Ard, R.W. Harvey, P.R. Johnson, *Environ. Sci. Technol.* 33 (1999) 63.
- [15] W.P. Johnson, B.E. Logan, *Water Res.* 30 (1996) 923.
- [16] Y. Sakagami, H. Yokoyama, H. Nishimura, Y. Ose, T. Tashima, *Appl. Environ. Microbiol.* 55 (1989) 2036.
- [17] E. Kiss, J. Samu, A. Toth, I. Bertoti, *Langmuir* 12 (1996) 1651.
- [18] S.F. Simoni, T.P. Bosma, H. Harms, A.B. Zehnder, *Environ. Sci. Technol.* 6 (2000) 1011.
- [19] D. Kiaie, A.S. Hlfman, T.A. Horbett, K.R. Lew, *J. Biomed. Mater. Res.* 29 (1995) 729.
- [20] K. Shellenberger, B.E. Logan, *Environ. Sci. Technol.* 36 (2002) 184.
- [21] T.L. Kurl, D.E. Leckband, D.D. Lasic, J.N. Israelachvili, *Biophys. J.* 66 (1994) 1479.
- [22] S. Abarzua, S. Jacobowski, *Mar. Ecol. Prog. Ser.* 123 (1995) 301.
- [23] H.C. Van der Mei, B. Van de Belt-Grittee, H.J. Busscher, *Colloids Surf. B: Biointerfaces* 5 (1995) 11.
- [24] G. Smit, M.H. Straver, B.J. Lugtenberg, J.W. Kijne, *Appl. Environ. Microbiol.* 58 (1992) 3709.
- [25] C.H. Bolster, A.L. Mills, G.M. Hornberger, J.S. Herman, *J. Contam. Hydrol.* 50 (2001) 287.
- [26] T.A. Camesano, B.E. Logan, *Environ. Sci. Technol.* 32 (1998) 1699.
- [27] M.C.M. van Loosdrecht, W. Norder, J. Lyklema, A.J. Zehnder, *Aquat. Sci.* 51 (1990) 103.
- [28] D.R. Absolom, F.V. Lamberti, A. Policova, W. Zingg, C.J. Van Oss, W. Neumann, *Appl. Environ. Microbiol.* 46 (1983) 90.
- [29] J. Gannon, Y. Tan, P. Baveye, M. Alexander, *Appl. Environ. Microbiol.* 57 (1991) 2497.
- [30] A. Zita, M. Hermansson, *Syst. Appl. Environ. Microbiol.* 60 (1994) 3041.
- [31] M. Hermansson, *Colloids Surf. B: Biointerfaces* 14 (1999) 105.
- [32] J. Azeredo, J. Visser, R. Oliveira, *Colloid Surf. B.* 12 (1999) 141.
- [33] S.F. Simoni, H. Harms, T. Bosma, A. Zehnder, *Environ. Sci. Technol.* 32 (1998) 2100.
- [34] Y.L. Ong, A. Razatos, G. Georgious, M.M. Sharma, *Langmuir* 15 (1999) 2719.
- [35] C.B. Greenberg, *Thin Solid Films* 251 (1994) 81.
- [36] C. Damm, F.W. Muller, G. Israel, S. Gablenz, H.P. Abicht, *Dye Pigment* 2 (2003) 151.
- [37] D. Cunliffe, C.A. Smart, C. Alexander, E.N. Vulfson, *Appl. Environ. Microbiol.* 65 (1999) 4995.
- [38] S.E. Truesdail, J. Lucasik, S.R. Farrah, D.O. Shah, R.B. Dickinson, *J. Coll. Interf. Sci.* 203 (1998) 369.
- [39] E.P. Knapp, J.S. Jeram, G. Heorberger, A.L. Millis, *Environ. Geol.* 33 (1998) 243.
- [40] A.L. Mills, J.S. Herman, G.M. Hornberger, T.H. DeJesus, *Appl. Environ. Microbiol.* 60 (1994) 3300.
- [41] R.T. Coughlin, S. Tonsager, E.J. McGroarty, *Biochemistry* 22 (1983) 2002.
- [42] B.A. Jucker, H. Harms, S.J. Hug, A.B.B. Zehnder, *Colloids Surf. B: Biointerfaces* 9 (1997) 331.
- [43] A. Razatos, Y.L. Ong, M.M. Sharma, G. Georgious, *Proc. Natl. Acad. Sci. U.S.A.* 95 (1998) 11059.
- [44] A. Razatos, Y.L. Ong, M.M. Sharma, G. Georgious, *J. Biomater. Sci. Polym. Ed.* 12 (1998) 1361.
- [45] G.A. Burks, S.B. Velegol, E.U. Watson, B.E. Lindenmuth, J.D. Feick, B.E. Logan, *Langmuir* 6 (2003) 2366.
- [46] M.F. DeFlaun, S.R. Oppenheimer, S. Streger, C.W. Condee, M. Fletcher, *Appl. Environ. Microbiol.* 65 (1999) 759.
- [47] B.R. Folsom, P.J. Chapman, P.H. Pritchard, *Appl. Environ. Microbiol.* 56 (1990) 1279.
- [48] A. Massol-Deya, R. Weller, L. Rios-Hernandez, J.Z. Zhou, R.F. Hickey, J.M. Tiedje, *Appl. Environ. Microbiol.* 1 (1997) 270.
- [49] D.L. Bedard, M.L. Haberl, *Microb. Ecol.* 20 (1990) 87.
- [50] F.J. Mondello, M.P. Turcich, J.H. Lobos, B.D. Erickson, *Appl. Environ. Microbiol.* 63 (1997) 3096.
- [51] B.D. Hoyle, L.J. Williams, J.W. Costerton, *Infect. Immun.* 61 (1993) 777.

- [52] K. Mathee, O. Ciofu, C. Sterberg, P.W. Lindum, J.I. Campbell, P. Jensen, A.H. Givskov, D.E. Ohman, S. Molin, N. Hoiby, A. Kharazmi, *Microbiology* 145 (1999) 1349.
- [53] B. Purevdorj, J.W. Costerton, P. Stoodley, *Appl. Environ. Microbiol.* 68 (2002) 4457.
- [54] T.T. Cloete, L. Jacobs, *Water SA* 1 (2001) 21.
- [55] M.R.W. Brown, J. Barker, *Trends Microbiol.* 7 (1999) 46.
- [56] G.A. O'Toole, R. Kolter, *Mol. Microbiol.* 30 (1998) 295.
- [57] P.K. Singh, A.L. Schaefer, M.R. Parsek, T.O. Moninger, M.J. Welsh, E.P. Greenberg, *Nature* 407 (2000) 762.
- [58] J.E. Hobbie, R.J. Daley, S. Jasper, *Appl. Environ. Microbiol.* 33 (1977) 1225.
- [59] J. Sieger, *Non Cryst. Solids* 19 (1975) 213.
- [60] F.K. Urban, P.Q. Athey, M.S. Islam, *Thin Solid Films* 253 (1994) 326.
- [61] P.Q. Athey, F.K. Urban, P.H. Holloway, *J. Vac. Sci. Tech.* 6 (1996) 3436.
- [62] C.B. Greenberg, *Ind. Eng. Chem. Res.* 40 (2001) 26.
- [63] C.B. Greenberg, *J. Electrochem. Soc.* 11 (1993) 3332.
- [64] K.C. Ho, D.E. Singleton, C.B. Greenberg, *J. Electrochem. Soc.* 137 (1990) 3858.
- [65] P.J. Stoodley, A.B. Boyle, I. Cunningham, H.M. Dodds, S. Lappin, Z. Lewandowski, *Biofilms in the Aquatic Environment*, The Royal Society of Chemistry Press, Cambridge, UK, 1999, p. 13.
- [66] R.E. Holm, P.H. Nielsen, H. Albrechtsen, T.H. Christensen, *Appl. Environ. Microbiol.* 58 (1992) 3020.
- [67] C.J. Van Oss, *Colloid Surf. A: Physicochem. Eng/Aspects* 78 (1993) 1.
- [68] J.A. Brant, A.E. Childress, *J. Membrane Sci.* 203 (2002) 257.
- [69] H.J. Busscher, A.H. Weerkamp, H.C. van der Mei, A.W. van Pelt, H. Long, J. Arends, *App. Environ. Microbiol.* (1984) 980.
- [70] H.J. Busscher, G.I. Geertsema-Doornbush, H.C. van der Mei, *J. Biomed. Mater. Res.* 34 (1997) 201.
- [71] C.J. van Oss, R.J. Good, M.K. Chaudhury, *J. Coll. Inter.* 111 (1986) 378.
- [72] H.C. van der Mei, J. de Vries, J. Busscher, *Surf. Sci. Rep.* 39 (2000) 1.
- [73] R.J. Hunter, *Foundations of Colloid Science*, vol. 1, Oxford University Press, New York, 1995.
- [74] J.H. Masliyah, *Electrokinetic Transport Phenomena*, AO STRA, Edmonton, Alberta, Canada, 1994.
- [75] S.L. Walkson, S. Bhattacharjee, E.M. Hoek, M. Elimelech, *Langmuir* 18 (2002) 2193.
- [76] J.A. Cleveland, S. Manne, D. Bocek, P.K. Hansma, *Rev. Sci. Instrum.* 64 (1993) 403.
- [77] S. Bhattacharjee, A. Sharma, P.K. Bhattacharya, *Langmuir* 10 (1994) 4710.
- [78] C.J. Van Oss, A. Docoslis, W. Wu, R.F. Giese, *Colloid Surf. B: Biointerface* 14 (1999) 99.
- [79] H.C. Hamaker, *Physica* 4 (1973) 1058.
- [80] J. Gregory, *J. Colloid Interface Sci.* 83 (1981) 138.
- [81] N.I. Abu-Lail, T.A. Camesano, *Environ. Sci. Technol.* 37 (2003) 2173.
- [82] S. Hong, M. Elimelech, *J. Membr. Sci.* 132 (1997) 159.
- [83] S. Bhattacharjee, A. Sharma, P.K. Bhattacharya, *Ind. Eng. Chem. Res.* 35 (1996) 3108.
- [84] L. Meagher, C. Klauber, R.M. Pashley, *Colloids Surf. A: Physicochem. Eng. Aspects* 106 (1996) 63.
- [85] M. Kastowsky, T. Gutberlet, H.J. Bradaczek, *Bacteriology* 174 (1992) 4798.
- [86] C.J. van Oss, *Interfacial Forces in Aqueous Media*, Marcel Dekker, New York, 1994.
- [87] M.J. Gross, B.E. Logan, *Appl. Environ. Microbiol.* 61 (1995) 1750.
- [88] D.G. Jewett, T.A. Hilbert, B.E. Logan, R.G. Arnold, R.C. Bales, *Water Res.* 29 (1995) 1673.
- [89] M. Elimelech, J. Gregory, X. Jia, R.A. Williams, *Particle Deposition and Aggregation: Measurement, Modeling, and Simulation*, Butterworth-Heinemann, Oxford, UK, 1995, p. 54.
- [90] H. Dong, T.C. Onstott, M.F. Deflaun, M.E. Fuller, T.D. Scherbe, S.H. Streger, R.K. Rothmel, B.J. Mailloux, *Environ. Sci. Technol.* 36 (2002) 891.
- [91] S.B. Velegol, B.E. Logan, *Langmuir* 19 (2002) 851.